Science of the Total Environment 651 (2019) 551–560

Contents lists available at ScienceDirect

Science of the Total Environment

journal homepage: www.elsevier.com/locate/scitotenv

Optimization and toxicity assessment of a combined electrocoagulation, H_2O_2/Fe^{2+}/UV and activated carbon adsorption for textile wastewater treatment

Edison GilPavas [a,*], Izabela Dobrosz-Gómez [b], Miguel-Ángel Gómez-García [c]

[a] GIPAB: Grupo de Investigación en Procesos Ambientales, Departamento de Ingeniería de Procesos, Universidad EAFIT, Cr 49 # 7 Sur 50, Medellín, Colombia
[b] Grupo de Investigación en Procesos Reactivos Intensificados con Separación y Materiales Avanzados - PRISMA, Departamento de Física y Química, Facultad de Ciencias Exactas y Naturales, Universidad Nacional de Colombia, Sede Manizales, Campus La Nubia, km 9 vía al Aeropuerto la Nubia, Apartado Aéreo 127, Manizales, Caldas, Colombia
[c] Grupo de Investigación en Procesos Reactivos Intensificados con Separación y Materiales Avanzados - PRISMA, Departamento de Ingeniería Química, Facultad de Ingeniería y Arquitectura, Universidad Nacional de Colombia, Sede Manizales, Campus La Nubia, km 9 vía al Aeropuerto la Nubia, Apartado Aéreo 127, Manizales, Caldas, Colombia

HIGHLIGHTS

- EC/H_2O_2/Fe^{2+}/UV process was evaluated for wastewater treatment.
- EC/H_2O_2/Fe^{2+}/UV performance was optimized by the Response Surface Methodology.
- Optimum conditions were found: pH = 4.3, [Fe^{2+}] = 1.1 mM and [H_2O_2] = 9.7 mM.
- EC/H_2O_2/Fe^{2+}/UV process yielded a colorless and highly mineralized effluent.

GRAPHICAL ABSTRACT

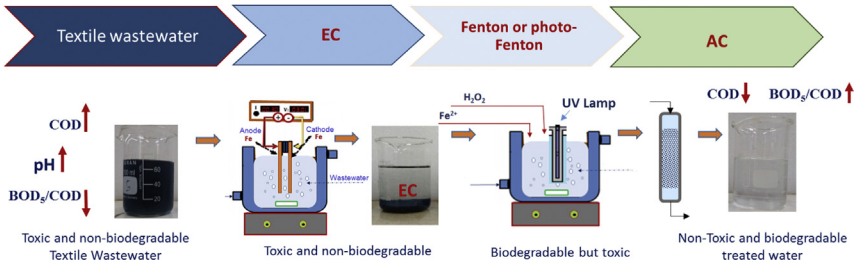

ARTICLE INFO

Article history:
Received 16 July 2018
Received in revised form 6 September 2018
Accepted 9 September 2018
Available online 11 September 2018

Editor: P Holden

Keywords:
Electrocoagulation
Fenton
Photo-Fenton
Activated carbon
Industrial textile wastewater
Optimization
Toxicity assessment

ABSTRACT

In this study, the potential application of sequential Electrocoagulation + Fenton (F) or Photo-Fenton (PF) + Active carbon adsorption (EC + F/PF + AC) processes were analyzed as alternatives for the treatment of an industrial textile wastewater resulting from an industrial facility located in Medellín (Colombia). In order to maximize the organic matter degradation, each step of the treatment was optimized using the Response Surface Methodology. At first, the optimal performance of EC was achieved with Fe electrodes operating at pH = 7, j_{EC} = 10 mA/cm^2 and 60 rpm, during 10 min of electrolysis. At these conditions, EC let to remove 94% of the dye's color, 56% of the COD and 54% of the TOC. Next, sequentially applied Fenton or photo-Fenton process (i.e., EC + F/PF), operating at the optimized conditions (pH = 4.3, [Fe^{2+}] = 1.1 mM, [H_2O_2] = 9.7 mM, stirring velocity = 100 rpm and reaction time = 60 min.), improved the quality of the treated effluent. The EC + F let to achieve total color reduction, as well as COD and TOC removals of 72 and 75%, respectively. The EC + PF reached 100% of color, 76% of COD and 78% of TOC reductions. The EC + F/PF processes were more efficient than EC in elimination of low molecular weight (<5 kDa) compounds from wastewater. Moreover, the BOD_5/COD ratio increased from 0.21 to 0.42 and from 0.21 to 0.46 using EC + F and EC + PF processes, respectively. However, EC + F/PF were not fully effective for the removal of acute toxicity to *Artemia salina*: 20% and 60% of reduction in toxicity using EC + F and EC + PF, respectively, comparing to very toxic (100%) raw textile wastewater. Thus, activated carbon adsorption was applied as an additional step to complete the treatment. After AC adsorption, the acute toxicity decreased to 10% and 0% using EC + F and EC + PF, respectively. The total operational costs, including chemical reagents, electrodes, energy consumption and sludge disposal, were of 1.65 USD/m^3 and 2.3 USD/m^3 for EC + F and EC + PF, respectively.

* Corresponding author.
E-mail addresses: egil@eafit.edu.co (E. GilPavas), idobrosz-gomez@unal.edu.co (I. Dobrosz-Gómez), magomez@unal.edu.co (M.-Á. Gómez-García).

https://doi.org/10.1016/j.scitotenv.2018.09.125
0048-9697/

1. Introduction

Textile industry consumes large quantities of water and produces large volumes of wastewater, mostly during dyeing and finishing processes. Textile wastewater is often rich in color. Moreover, it is characterized with the presence of residues of reactive dyes and other hardly-degradable chemicals as well as high concentrations of Chemical Oxygen Demand (COD) and Biological Oxygen Demand (BOD_5). Textile dyes are mainly aromatic and heterocyclic compounds. Their complicated and stable structure includes color-display and polar groups, both hardly-degradable. Indeed, the toxic effect of dyestuffs on both living species and the aqueous environment is widely recognized (Villanueva-Rodríguez et al., 2009; Shaolan Ding et al., 2010).

Throughout the world, the discoloration and degradation of textile wastewater is mandatory before its final disposal. In fact, the latest environmental regulations have required the development of alternative treatment techniques to meet the standards. It has been proven that physico-chemical processes (*v. g.*, coagulation/flocculation, precipitation, adsorption, ion exchange, membrane separation and oxidation) result in incomplete mineralization of pollutants (Zhou et al., 2009). On the other hand, in many cases, due to the toxicity of textile wastewater, biological methods are inefficient especially if the pollutants are present in high concentrations (Ghanbari and Moradi, 2015). Recently, electrochemical technologies (such as electrocoagulation, electroflotation, electrodecantation, electrooxidation, etc.…) and Advanced Oxidation Processes (AOPs) have been considered as efficient alternatives for textile wastewater remediation (Brillas and Martínez-Huitle, 2015). The combination of these processes have been successfully applied for the treatment of several types of wastewaters. Sequential electrocoagulation/electrochemical Fenton (Flores et al., 2018) and coagulation/acid cracking/Fenton process (Yazdanbakhsh et al., 2015) were used for the treatment of olive oil mill wastewater. The sequential permanganate, electro-Fenton and Co_3O_4/UV/peroxymonosulfate (Jaafarzadeh et al., 2017) process was applied for pulp and paper resulting wastewater. An integrated electrocoagulation-electrooxidation (Ibarra Taquez et al., 2017) was used to treat wastewater resulting from a soluble coffee plant. Finally, combination of coagulation/photocatalytic methods (Jorfi et al., 2016) was also considered for dye and real textile wastewater treatment. In all these cases, the arrangement of different treatment processes improved global wastewater characteristics, minimized operational costs, slightly providing into no generation of secondary recalcitrant wastes and letting to obtain treated effluents with appropriate quality to be discharged into water bodies.

In this work, the potential application of a sequential EC + (Fenton (F) or photo-Fenton (PF)) + AC adsorption process is analyzed as an alternative for the treatment of an industrial textile wastewater (ITWW). First, electrocoagulation (EC) is used. It is a very versatile method for water and wastewater remediation. It has been successfully applied to remove a wide variety of pollutants, among them heavy metals, different anions and organic compounds including dyes (Kobya et al., 2003; Garcia-Segura et al., 2017; Vepsalainen et al., 2011). EC presents many advantages over other techniques, such as high efficiency at low capital and operational costs, equipment simplicity and easiness of process control. It relies on the electrochemical dissolution of a sacrificial metal electrode (usually made of iron or aluminum) into soluble or insoluble species that enhance the coagulation, the adsorption or the precipitation of soluble or colloidal pollutants (Mollah et al., 2004). Pollutant nature and concentration, electrode material, current density, solution pH and electrolyte type are known as factors influencing the effectiveness of EC treatment. The following reactions describe the processes involved in EC, if iron electrodes are used:

At the anode:

$$Fe_{(s)} \rightarrow Fe^{2+}_{(aq)} + 2e^- \quad (1)$$

$$4\,Fe^{2+}_{(aq)} + 10H_2O_{(l)} + O_{2(g)} \rightarrow 4\,Fe(OH)_{3(s)} + 8H^+ \quad (2)$$

At the cathode:

$$4H^+_{(aq)} + 4e^- \rightarrow 2H_{2(g)} \quad (3)$$

It is important to notice that H_2 generation can provide an extra removal of organic material by flotation.

On the other hand, AOPs deal with the use of hydroxyl radicals (•OH) to attack the pollutant molecules present in wastewater. They are recognized as valuable methods to increase the biodegradability of textile wastewater due to its high oxidative efficiency. A variety of AOPs have been reported in the literature, among them UV/H_2O_2, UV/O_3 (Boczkaj and Fernandes, 2017), TiO_2-assisted photocatalysis, Fenton process (Fe^{2+}/H_2O_2) (De Lima et al., 2017; Rosa et al., 2015), electrochemical AOPs (Chatzisymeon et al., 2006) and ultrasonication (Darvishi et al., 2016). The Fenton oxidation is an attractive method to mineralize dyes remaining in textile wastewater. Indeed, H_2O_2 is an environmentally friendly oxidant, which is decomposed into water and oxygen, and iron is highly abundant and presents low toxicity (Ghanbari and Moradi, 2015). Fenton processes exhibit the following advantages: equipment simplicity, relatively low cost and easy operation and maintenance (Zazo et al., 2005). Moreover, due to its non-selectivity nature, it provides the removal of wide spectrum of contaminants together with a dramatic reduction in toxicity (Arzate-Salgado et al., 2016). The coupling of EC and Fenton process has been shown to be highly effective due to the generation of strongly oxidizing species. In this case, the electrocoagulated water (i.e., the resulting supernatant) can be further subjected to Fenton or photo-Fenton process. During Fenton reaction, H_2O_2 decomposition is catalyzed by ferrous ion to generate hydrous radicals (•OH) according to Eq. (4) (El-Ghenymy et al., 2012):

$$Fe^{2+} + H_2O_2 \rightarrow Fe^{3+} + HO^{\cdot} + HO^- \quad (4)$$

The highly reactive •OH radicals can in turn react with dyes present in wastewater, resulting in their oxidation. The Fe^{3+} ion can be recycled via Eq. (5), but this process is relatively slow (Rahim Pouran et al., 2015).

$$Fe^{3+} + H_2O_2 \rightarrow Fe^{2+} + \dot{HO_2} + H^+ \quad (5)$$

It has been established that photo-Fenton reaction can further improve the degradation of organic pollutants, either by direct photolysis or by increasing the production of •OH radicals, according to the following reactions (GilPavas et al., 2017):

$$Fe^{3+} + H_2O_2 \rightarrow Fe(HO_2)^{2+} + H^+ \quad (6)$$

$$Fe(HO)^{2+} + h\nu \rightarrow Fe^{2+} + HO^{\cdot} \quad (7)$$

Unfortunately, the partial oxidation of organic contaminants may also result in the formation of toxic intermediates (even more noxious than the parent compounds). In such a case, an additional treatment must be applied to the resulting effluent prior to its final disposal into the aqueous environment.

Adsorption processes are commonly used as a final step in the treatment of industrial wastewater. Activated carbon (AC) has been proven as an efficient adsorbent for the removal of a wide variety of environmental pollutants. Indeed, harm by-products (v.g., volatile, semi-volatile and non-volatile chlorinated organic pollutants) can be removed by AC adsorption even at very low concentration levels (Lemus et al., 2012; Pavoni et al., 2006). Among the unique properties of AC, the following can be mentioned: (i) high specific surface area; (ii) easy and wide availability; (ii) stability in acidic/basic environment; and (iv) structural stability at high temperatures. Thus, final adsorption

step, using AC, is expected to reduce the toxicity of the wastewater generated after EC + F or EC + PF processes.

It is important to notice that most of the studies reported in the open literature for textile wastewater treatment uses synthetic textile wastewater (i.e., dye dissolution in the distilled water). In this work, the use of an ITWW sample involves additional challenges such as presence of mixed pollutants and auxiliary chemicals used during the dyeing process. Additionally, many other factors such as turbidity, high chloride content and pH can also affect the performance of the final wastewater treatment. Thus, at the beginning, the raw effluent was characterized for organic matter content (Total Organic Carbon (TOC), Chemical Oxygen Demand (COD), and Biological Oxygen Demand (BOD_5)), solids amount (Total solids (TS), Turbidity), Conductivity (κ), biodegradability (BOD_5/COD ratio) and toxicity (mortality of *Artemia salina*). Then, the influence of different operational conditions (for EC: pH, current density and stirring velocity; and for F and PF processes: Fe^{2+} concentration, H_2O_2 concentration and pH) on the efficiency of EC + F or EC + PF processes (removal of: color, COD, TOC and turbidity) was evaluated. They were optimized using a Box-Behnken experimental Design (BBD) and Response Surface Methodology (RSM). The optimal operational conditions were validated experimentally.

2. Materials and methods

2.1. Samples handling and analytical methods

ITWW samples were collected from an equalization tank in a textile industrial plant located in Medellin-Colombia. This facility produces denim jeans and generates ca. 800 m^3/day of wastewater. It presents dark blue color due to the mixture of several dyes (v.g., reactive, direct, dispersive, acid and cuba dyes) as well as other pollutants used during the textile processing. ITWW samples were kept refrigerated, to avoid compounds degradation during storage and transportation, following APHA's standard procedures (Apha, 2012).

Raw samples and these resulting from the laboratory tests were analyzed by triplicate. Standard methods were followed for the quantitative analysis of color (Method 2120B, using UV–Vis double-beam spectrophotometer, Spectronic Genesys 2PC, in the range of 200–700 nm, with a 1 cm path length quartz cell. It is important to mentioned that before color measurements, samples were first centrifuged and then filtered (using 0.45 μm membrane) in order to eliminate any turbidity that can interfere with color analysis following 7887 BCE protocol), total solids (Method 2130B), COD (closed reflux method with colorimetric determination, Method 5220D), TOC (Method 5310D) and BOD_5 (the respirometric method, 5210B). H_2O_2 concentration was measured by iodometric titration. To avoid the interference of H_2O_2 during COD measurements, the residual H_2O_2 was quenched using MnO_2 (Sigma Aldrich; reagent grade ≥ 90%). All reagents were used as received from suppliers without any further purification ($FeSO_4.7H_2O$ (99 wt%) and H_2O_2 (30 vol%)). Their aqueous solutions were prepared using ultrapure water (Milli-Q system, Billerica, Massachusetts; conductivity <1 μS/cm). Their pH values were adjusted with sulfuric acid (H_2SO_4; Merck, 98 vol%) or sodium hydroxide (NaOH, Carlo Erba, purity = 97 vol%).

The Molecular Weight Distribution Analysis (MWDA) of representative samples was performed by the membrane ultrafiltration method (Ibarra Taquez et al., 2017), using a stirred cell with cellulose ultrafiltration membranes (Amicon, Model 8400, membranes of 44.5 mm, Millipore Corporation, Germany) with nominal molecular weight limits (NMWL) of 30, 10, 5 and 3 kDa. The operational pressure of ultrafiltration, provided by steady supply of highly pure N_2 (99.99 vol%), was 0.2 MPa. Before using, membranes were washed for 30 min with 0.1 M NaOH, flushed with deionized water and preserved in 10% ethanol/water solution at 4 °C, according to the manufacturer instructions. The initial and final 5 mL of filtrate from each ultrafiltration process were discarded due to membrane fouling. Afterwards, TOC was analyzed for each molecular weight fraction.

Generated carboxylic acids were quantified by ion-exclusion high performance liquid chromatography (HPLC, Agilent 1200), using a Hi-Plex column (300 mm × 7.8 mm, at 35 °C) and setting the photodiode array detector at λ = 210 nm. These measurements were made by injecting 20 μL aliquots into the LC and using a mobile phase of 4 mM H_2SO_4 at 0.6 mL/min. The chromatograms displayed well-defined peaks at residence time values of 7.2 min. For oxalic acid, 9.65 min. for tartaric acid, 11 min. for malonic acid and 14.9 min. For formic acid.

Toxicity essays were performed evaluating the immobilization of *Artemia salina* (*A. salina*, Carolina Biological Supply Company, USA) for both original ITWW effluent and after-treatment samples. The *A. salina* were bred in an aqueous culture medium whose salinity resembled the conditions for the survival and development of these microcrustaceans (Da Costa Filho et al., 2016). Test plates containing 20 crustaceans in 9.5 mL of sample solution and 0.5 mL of saline medium were incubated for 24 h at 25 ± 1 °C. Lateral illumination by a light tube (3500 Lux) was supplied during the test period. No food was given to these crustaceans between hatching and test steps. Acute toxicity was assessed by noting the effects of the test-compounds on the mobility of *A. salina*. The crustaceans were considered immobile if after 24 h of incubation they remained at the bottom of the test container and did not start swimming within 15 s of observation. Acute toxicity was expressed as percentage of immobilization compared to a nontoxic control, where an artemia immobilization of 10% is accepted after 24 h of exposure. The mortality of *A. salina* was calculated with the following equation:

$$\text{Mortality}\ (\%) = \left(\frac{N_0 - N_t}{N_0}\right) \times 100 \tag{8}$$

where, N_0 and N_t are the number of crustaceans originally taken and the number of crustaceans alive after exposure to after-treatment sample for a period of time (t), respectively.

2.2. Experimental set-up and procedure

For EC experiments, a plexiglass, continuously stirred, batch jacketed reactor with 100-mL working volume was used. It contained two vertical plate, iron made electrodes (pure iron content >98%; dimensions of 18 mm width, 50 mm height and 0.6 cm thickness) in a monopolar arrangement to a DC power source (BK-Precision, 0–30 V, 0–5 A, Yorba Linda, California), operating in galvanostatic mode. The gap between them was set up at 1 cm. On the top of the cell, a PT-100 sensor (± 0.01 °C) was placed to measure solution temperature. All experiments were performed at 22 °C (±0.01 °C), regulated using a Polyscience 712 thermostat (Niles, Illinois) connected to the reactor jacket. Before each run, the electrodes were rubbed with sand paper and dipped in a 30 vol% H_2SO_4 solution to remove impurities from their surface. Then, they were rinsed with distilled water before the experiment.

EC experimental conditions were previously optimized (not shown here) by Response Surface Methodology (RSM). It was found that iron is more efficient in neutral and alkaline medium, especially at pH between 6 < pH < 9 (similar results were also reported by Kobya et al. (2003)). Thus, for all experiments, pH of 7 and stirring velocity of 60 rpm were used. To determine the amount of sludge formed during EC, the effluent was filtered and solid residue was dried until constant weight. Then, filtered solution was treated by Fenton or Photo-Fenton process.

Fenton reaction was carried out in a continuously stirred glass reactor with 80 mL working volume. The PF process used a 150 mL total volume cylindrical quartz reactor, with an internal annular devise where a UV radiation lamp was placed. A black-light tubular lamp was used (maximum light intensity at λ = 365 nm, 15 mm of diameter, 225 mm of length, model F6T5/BL Philips, 6 W, photon flux of 1.47

$\times 10^{19}$ 1/m^2/s, radiant flux of 0.5 mW/cm^2). The radiation flux was measured using a Delta Ohm HD 2102 radiometer and the total irradiated area was of 100 cm^2. The reaction time was kept at 45 min. For all experiments, the solution was stirred with a magnetic bar to ensure its homogenization and to avoid mass transfer resistance effects. The initial solution pH was adjusted with diluted H_2SO_4 and measured by pH meter. At the end of each run, a 5 mL sample was taken and centrifuged at 2000 rpm for 10 min before analysis.

After (EC + F) or (EC + PF) treatment, resulting effluent was passed through a granular activated carbon bed (AC, WPH, Calgon Carbon, Pittsburgh, PA., mesh 10), in order to eliminate any toxic compounds. Before each run, the AC was rinsed with extra-pure water (Milli-Q System), and baked at 175 °C for 1 week to remove volatile impurities. AC was kept in the oven at 105 °C. Before its use, the AC was moved into a desiccator to let it cool down to room temperature. Adsorption was conducted in a glass column with inner diameter of 28 mm and effective length of 120 mm. The flow rate was 20 mL/min at 25 °C with a retention time of 3.7 min and the loading amount of AC in the column was 45 g. After the adsorption process, the effluent was filtered through a 0.45 μm membrane filter; finally, the acute toxicity was analyzed.

2.3. Experimental design and statistical analysis

(EC + F) and (EC + PF) process efficiencies were investigated by means of three level Box-Behnken experimental Design (BBD) and optimized (i.e., maximizing the organic matter degradation) using RSM. Independent variables and their levels were selected from preliminary experiments (GilPavas et al., 2017) as follows: (i) Fe^{2+} concentration: in the range of 0.7–2.7 mM; (ii) H_2O_2 concentration: ranging from 9.7–38.82 mM and (iii) pH, between 3 and 6. All experiments were made by triplicate and the average value of each response variable (i.e., COD and color removal percentage (%DCOD, %DC Eqs. (9)–(10) were used for statistical analysis:

$$\%\mathrm{DCOD} = \frac{\mathrm{COD_i} - \mathrm{COD_t}}{\mathrm{COD_i}} \times 100 \tag{9}$$

where COD_i and COD_t represent the COD concentration of wastewater sample before (time zero) and after treatment (total time of analysis), respectively (in g/L).

The percentage of color removal was also measured according to Eq. (10):

$$\textit{Color removal}\ (\%DC) = \frac{(\mathrm{Abs_i} - \mathrm{Abs_t})}{\mathrm{Abs_i}} \times 100 \tag{10}$$

where, Abs_i and Abs_t are absorbance before and after treatment, respectively, measured at 660 nm.

In order to define the economic feasibility of the process, operating costs (OC) were calculated as follows:

$$OC_{EC}\left(\frac{USD}{m^3}\right) = \frac{1}{V_{r1}}\left(1.08\frac{MIt}{nF} + 0.1867VIt + 0.010D\right) \tag{11}$$

$$OC\left(\frac{USD}{m^3}\right) = \left(OC_{EC} + \frac{1}{V_{r2}}(0.0012t + 0.4I + 0.5P + 0.28S)\right) \tag{12}$$

where OC_{EC} is the EC operating cost, Vr_1 (m^3) is the reaction volume of EC and Vr_2 (m^3) is the reaction volume of F or PF stages. The first term in the parenthesis of Eq. (11) represents the cost of the anode consumed during EC (USD/kg), determined using Faraday's law with a safety factor of 20% (i.e., Faraday's law values is multiplied by 1.2), M is the molecular weight (kg/kmol) of anode material, I is the electric current (A), t is the electrolysis time (h), n is the amount of electrons transferred, and F is Faraday's constant (26,801.4 Ah/kmol.) The second and third terms correspond to the energy spent during the process, with V as the applied voltage (V) and D the amount of generated sludge (kg). In Eq. (12), 0.0012 is the energy consumption (kW) of the applied lamp; I, P and S is the amount (kg) of $FeSO_4.7H_2O$, H_2O_2 and H_2SO_4 used during experiments, respectively. OC were calculated using statistics data for 2017 provided by Colombian official agency (i.e., anode's material cost = 0.9 USD/kg, energy cost = 0.2 USD/kWh, $FeSO_4.7H_2O$ cost = 0.4 USD/kg, H_2O_2 cost = 0.5 USD/kg, H_2SO_4 cost = 0.28 USD/kg, and solids disposal cost = 10 USD/ton).

Experimental design results were adjusted to a second-order model as in Eq. (13) using Statgraphics Centurion XVI Software:

$$Y_i = \beta_0 + \sum_{i=1}^{3}(\beta_i X_i) + \sum_{i=1}^{3}\left(\beta_{ii}{X_{ii}}^2\right) + \sum_{i=1}^{3}\cdot\sum_{j=1}^{3}\left(\beta_{ij}X_iX_j\right) \tag{13}$$

where β_0, β_i, β_{ii}, β_{ij} are the regression coefficients for the intercept, linear, square, and interaction terms, respectively; and X_i and X_j are independent variables. The quality of the model and capacity to estimate experimental results was assessed with the adjusted determination coefficient, R^2_{adj}. Details of this methodology have been reported elsewhere (GilPavas et al., 2017; Ghanbari and Moradi, 2015).

3. Results and discussion

A summary of ITWW characteristics together with the Colombian emission limits are presented in Table 1. Notice that pH, COD, and BOD_5 values do not fulfill Colombian environmental regulations. The ITWW shows an intense blue color mainly due to the presence of indigo dye, inferring a high loading of organic compounds. Moreover, it presents high conductivity due to the presence of different soluble salts. High COD value, more than twice of that of the permissible limit, implies the presence of large amounts of non-biodegradable organic matter. Actually, the initial BOD_5/COD ratio of 0.21 (<0.4) indicates that the effluent is not biodegradable (GilPavas et al., 2017).

3.1. The efficiency of EC for ITWW treatment

The evolutions of color, COD and TOC removal and the OC of wastewater treated by EC are presented in Fig. 1. The significant improvement in wastewater quality, equivalent to 56% of COD, 54% of TOC, 94% of color and 92% of turbidity removals, was observed at the following electrolysis conditions: current density = 10 mA/cm^2, pH = 7 and electrolysis time = 10 min (previously optimized conditions). A summary of the complete characterization of EC resulting supernatant is presented in Table 1. During EC, chloride is anodically converted to active chlorine, which can oxidize the dye leading to its decolorization (Emamjomeh and Sivakumar, 2009). The EC process was able to eliminate (almost completely) the turbidity and to reduce organic loading. However, it failed to achieve COD discharge limits (it was inefficient in removing surfactants and other soluble organic pollutants). Indeed, the biodegradability ratio BOD_5/COD increased slightly from 0.21 to 0.27, still presenting a very low value (<0.4) and indicating that it cannot be considered as biodegradable. Moreover, the acute toxicity of wastewater after EC treatment did not decrease. This implies that an additional wastewater treatment is required before its final discharge into the surface waterbodies. Thus, Fenton and photo-Fenton processes were evaluated as alternatives to complete the ITWW handling and to reach the permissible legislation discharge limits.

3.2. Fenton (F) and photo-Fenton (PF) processes for EC supernatant treatment

Fenton (F) and photo-Fenton (PF) processes was individually applied to reduce COD concentration and to increase the biodegradability of the effluent resulting from EC process. The BBD and RSM analysis were used to determine the individual effects of F or PF operational parameters (v.g., [Fe^{2+}], [H_2O_2] and initial pH) and their interactions on

Table 1
Physico-chemical parameters of raw ITWW together with global operating costs of treatment using different methods: EC, EC + F, EC + PF, EC + F + AC and EC + PF + AC.

Parameter	ITWW sample	Permisible limit[a]	After EC	After EC + F	After EC + PF	After EC + F + AC	After EC + PF + AC	Global treatment efficiency (%)			
								EC + F	EC + PF	EC + F + AC	EC + PF + AC
pH	8.2	6–9	7.6	5.3	4.0	6.5	5.9	–	–	–	–
Conductivity (mS/cm)	5.04	–	5.1	5.2	5.3	5.0	5.1	–	–	–	–
Absorbance (660 nm)	1.9	–	0.11	0	0	0	0	100	100	100	100
Color (Pt-Co units)	1399	–	366	53	44	49	40	96	97	96.5	97
Total solids (g/L)	0.62	–	0.14	0.0	0.0	0.0	0.0	100	100	100	100
COD (mg O_2/L)	970	400	430	274	238	262	226	72	76	73	77
TOC (mg C/L)	220	–	102	55	48	47	42	75	78	79	81
BOD_5 (mg O_2/L)	206	200	116	115	109	113	108	44	47	45	48
BOD_5/COD ratio	0.21	0.5	0.27	0.42	0.46	0.43	0.48	–	–	–	–
Mortality (%)	100	–	100	80	40	10	0.0	–	–	–	–
Generated sludge (kg/m^3)	–	–	0.98	0.98	0.98	0.98	0.98	–	–	–	–
Operating costs (USD/m^3)	–	–	0.63	1.65	2.3	–	–	–	–	–	–

[a] Emission limit values for industrial wastewater discharges into the municipal sewer system according to Res 0631, 17/03/2015, issued by the Ministry of Environment and Sustainable Development, Colombia.

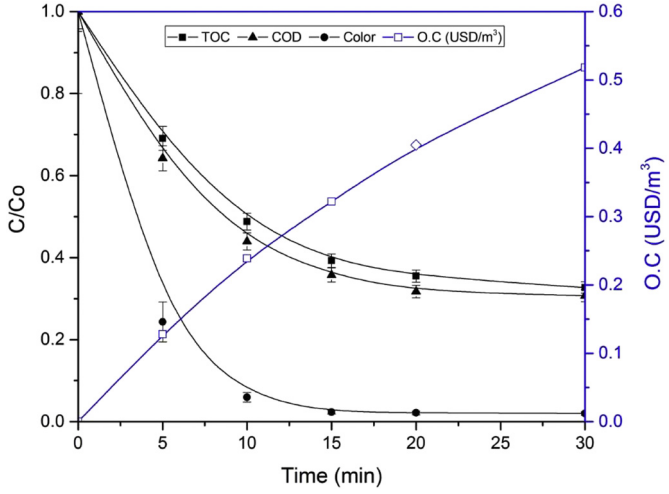

Fig. 1. The evolution of color, COD and TOC removals and the OC of wastewater treated by EC process. Experimental conditions: Fe anode, Fe cathode, j_{EC} = 10 mA/cm^2, pH = 7, stirring velocity = 60 rpm.

processes efficiencies (v.g., defined response variables: %DC, %DCOD and OC). The experimental design together with the obtained results are presented in Table 2. Notice that for EC + F process, the percentage of color removal varied between ca. 82 and 96% while the %DCOD varied between ca. 14 and 38%; with OC ranging from ca. 1.3 to 4.9 USD/m^3.

On the other hand, for the EC + PF process, the %DC varied in the range of ca. 82 to 99%, the COD reduction varied between ca. 19 and 50%, with OC varied from ca. 1.6 to 5.18 USD/m^3. To optimize the F and PF operating conditions (i.e., both to maximize %DCOD and to minimize OC), %DC, %DCOD and OC data were adjusted to second order polynomial models (Eqs. (14) to (19)). Model predictions matched accurately to the experimental results, with the following determination coefficients: (i) for F: R^2 = 0.983 for %DC and R^2 = 0.966 for %DCOD; and (ii) for FP: R^2 = 0.990 for %DC and R^2 = 0.975 for %DCOD (Table 3).

For Fenton process:

$$\%DC = 67.86 + 11.46 \times pH - 0.0203 \times H_2O_2 + 2.011 \times Fe^{2+} - 1.96 \times pH^2 + 0.1 \times pH \times H_2O_2 + 1.81 \times pH \times Fe^{2+} - 0.011 \times (H_2O_2)^2 + 0.009 \times H_2O_2 \times Fe^{2+} - 1.94 \times \left(Fe^{2+}\right)^2 \quad (14)$$

$$\%DCOD = -101.55 + 57.53 \times pH - 0.2828 \times H_2O_2 + 16.98 \times Fe^{2+} - 6.46 \times pH^2 + 0.067 \times pH \times H_2O_2 - 1.36 \times pH \times Fe^{2+} - 0.0068 \times (H_2O_2)^2 + 0.12 \times H_2O_2 \times Fe^{2+} - 2.9 \times \left(Fe^{2+}\right)^2 \quad (15)$$

$$OC\left(\frac{USD}{m^3}\right) = 0.125 + 0.0133 \times pH + 0.1134 \times H_2O_2 + 0.15 \times Fe^{2+} - 0.0044 \times pH^2 \quad (16)$$

Table 2
The experimental results on %DC, %DCOD and OC, according to the BBD for F and PF processes. Reaction time: 45 min.

				Fenton (F)			Photo-Fenton (EC + PF)		
Run	pH	H_2O_2 (mM)	Fe^{2+} (mM)	%DC (Pt-Co)	DCOD (%)	OC (USD/m^3)	%DC (Pt-Co)	DCOD (%)	OC (USD/m^3)
1	4.5	38.82	2.7	94.81	36.05	4.90	98.91	50.00	5.18
2	4.5	9.7	2.7	95.90	37.21	1.60	86.34	41.28	1.88
3	6	9.7	1.7	87.43	18.02	1.40	92.62	24.42	1.68
4	4.5	38.82	0.7	86.89	26.74	4.60	92.35	29.07	4.88
5	4.5	9.7	0.7	88.52	34.88	1.30	93.17	36.28	1.58
6	6	24.26	2.7	95.36	23.26	3.20	95.08	31.40	3.48
7	3	24.26	2.7	91.00	27.91	3.28	92.00	39.53	3.56
8	3	24.26	0.7	89.00	13.95	2.98	91.00	29.07	3.26
9	3	9.7	1.7	94.54	27.91	1.48	81.69	32.56	1.76
10	4.5	24.26	1.7	95.36	38.37	3.10	97.54	44.19	3.38
11	6	38.82	1.7	87.98	19.19	4.70	93.17	24.42	4.98
12	4.5	24.26	1.7	95.90	38.84	3.10	96.99	42.79	3.38
13	3	38.82	1.7	86.34	23.26	4.78	91.53	24.42	5.06
14	6	24.26	0.7	82.51	17.44	2.90	96.99	18.84	3.18
15	4.5	24.26	1.7	96.17	36.98	3.10	97.27	41.86	3.38

For Photo-Fenton process:

$$\%DC = 41.21 + 17.52 \times pH + 1.26 \times H_2O_2 - 4.34 \times Fe^{2+} - 1.43 \times pH^2 - 0.1064 \times pH \times H_2O_2 - 0.1517 \times pH \times Fe^{2+} - 0.0203 \times (H_2O_2)^2 + 0.23 \times H_2O_2 \times Fe^{2+} - 0.2796 \times \left(Fe^{2+}\right)^2 \quad (17)$$

$$\%DCOD = -59.28 + 46.81 \times pH - 0.135 \times H_2O_2 - 1.19 \times Fe^{2+} - 5.76 \times pH^2 + 0.093 \times pH \times H_2O_2 + 0.35 \times pH \times Fe^{2+} - 0.0166 \times (H_2O_2)^2 + 0.2737 \times H_2O_2 \times Fe^{2+} - 0.2671 \times \left(Fe^{2+}\right)^2 \quad (18)$$

$$OC\left(\frac{USD}{m^3}\right) = 7.13 + 0.0133 \times pH + 0.1134 \times H_2O_2 + 0.15 \times Fe^{2+} - 0.0044 \times pH^2 \quad (19)$$

The ANOVA was used to determine statistical significance of main factors and their interactions. It consists of classifying and cross-classifying statistical results, decomposing the contribution of each variable (or factors) and their double-interactions in the variance of each response variable. The *p*-values were used to identify the experimental parameters that have statistical influence on a particular response. If a *p*-value was lower than 0.05, it was considered that the specific variable shows statistical significance within the 95% confidence level. The ANOVA results are presented in Table 3.

Examining *p*-values, it can be seen that there are some variables and their interactions that are statistically significant (i.e., $p > 0.05$) for color and COD removals. In the case of F process, only the interaction $[H_2O_2]$-$[Fe^{2+}]$ is not statistically significant for %DC; while for %DCOD, only $[Fe^{2+}]$ and the quadratic term of pH-pH interaction are significant. On the other hand, for PF process, the statistically significant factors for %DC are $[Fe^{2+}]$, its quadratic term as well as the interaction pH-$[Fe^{2+}]$; whereas for %DCOD, the factors are pH, $[Fe^{2+}]$, the quadratic terms of pH-pH, $[H_2O_2]$-$[H_2O_2]$ and the interaction of $[H_2O_2]$-$[Fe^{2+}]$.

As expected, the factors that presented the major effect on %DCOD were H_2O_2 and iron concentrations. Indeed, proper $[H_2O_2]$ and $[Fe^{2+}]$ are important during Fenton process (Domínguez et al., 2012). Their excess or deficiency can considerably decrease process efficiency (Bautitz and Nogueira, 2007). In Fenton and photo-Fenton processes, the presence of H_2O_2 is essential, considering that it is the main source of •OH radicals for the oxidation process (Bobu et al., 2008). However, due to the radical scavenging effect of H_2O_2, the auto-decomposition of H_2O_2 (to O_2 and H_2O) and the fact that high concentrations of H_2O_2 may reduce the COD removal efficiency (see Table 2), the optimal concentration of H_2O_2 should be determined for each Fenton processes. In addition, the use of appropriate concentrations of reagents will prevent extra costs of operation, which may result from the use of excess reagents and will reduce the difficulties of removing iron excess (Zazo et al., 2011). Notice that low OC was obtained at low Fe^{2+} concentration and high pH values, which were almost the opposite conditions for higher degradation efficiency. Therefore, the integrated influence of operational parameters on degradation efficiency and OC should be considered to determine operating conditions for Fenton or photo-Fenton processes.

Table 3
The ANOVA for the %DC, %DCOD and OC as a function of pH (A), $[H_2O_2]$ (B) and $[Fe^{2+}]$ (C), according to the BBD.

	Fenton (F)		Photo-Fenton (PF)	
DC (%)	*F* value	*P* value	*F* value	*P* value
A:pH	7.52	0.0406	105.10	0.0002
B:$[H_2O_2]$	14.01	0.0134	110.01	0.0001
C: $[Fe^{2+}]$	118.41	0.0001	2.27	0.1923
AA	74.49	0.0003	68.72	0.0004
AB	19.95	0.0066	38.74	0.0016
AC	30.67	0.0026	0.37	0.5687
BB	21.02	0.0059	122.26	0.0001
BC	0.08	0.7939	80.47	0.0003
CC	14.52	0.0125	0.52	0.5039
R^2/R^2_{adj} (%)	98.30/95.24		99.04/97.31	
DCOD (%)	*F* value	*P* value	*F* value	*P* value
A:pH	4.10	0.0988	15.40	0.0111
B:H_2O_2	2.93	0.1478	0.96	0.3713
C:Fe^{2+}	17.70	0.0084	52.53	0.0008
AA	111.69	0.0001	108.94	0.0001
AB	1.21	0.3207	2.91	0.1490
AC	2.38	0.1839	0.19	0.6785
BB	1.10	0.3414	8.03	0.0365
BC	1.75	0.2435	11.13	0.0206
CC	4.45	0.0887	0.05	0.8383
R^2/R^2_{adj} (%)	96.63/93.57		97.52/93.06	

Response surface plots were used to analyze the simultaneous effects of two factors over each response variable. They were constructed from Eqs. (14) to (19) for a fixed $[H_2O_2]$ of 9.7 mM (Fig. 2). For F and PF processes, respectively, Fig. 2(a) and (b) show the effect of Fe^{2+} concentration and pH on the color removal and Fig. 2(c) and (d) on COD removal efficiencies. As it can be seen, almost complete color removal was accomplished with both processes. It should be mentioned that the decolorization rate increases if Fe^{2+} concentration increases (Fig. 2 (a) and (b)). Such behavior indicates that dye elimination involves ferrous ion initiation that is accelerated by H_2O_2 decomposition, Eqs. (4) and (6). Hydroxyl radicals, •OH, are able to attack quickly the organic substrates, causing their chemical decomposition by H-subtraction and addition to C = C unsaturated bonds. In the case of % DCOD, Fig. 2(c) and (d), maximal efficiency was achieved at intermediate pH values. In fact, at high pH values, iron precipitates as hydroxide ($Fe(OH)_3$) and, in this form, it decomposes H_2O_2 into water and oxygen. As a result, less hydroxyl radicals will be available for the oxidation process. Additionally, at lower pH, oxonium ion $(H_3O)^+$ formation enhances H_2O_2 stability, restricting •OH radical generation, resulting in lower dye degradation efficiency. The highest %DCOD was obtained using PF process which corresponds with the lower pH value (Table 2). In fact, it is well known that low pH values allow both higher solubility and higher UV radiation absorption capacity of iron species (Malato et al., 2009). Fig. 2(e) and (f) show the effect of pH and Fe^{2+} concentration on OC for F and PF processes, respectively. In both cases, it was found that the OC values increase with an increase in Fe^{2+} and H_2O_2 concentrations, at low pH values (in disagreement with the results that maximize both the reduction of color and COD). Thus, an optimization problem was formulated. It consisted of the determination of the minimal attainable OC to achieve a %DCOD higher than a specific desired value (i.e., 40% in accordance with Colombian environmental legislation limits – Table 1). It includes Eqs. (16) and (19), coupled with Eqs. (15) and (18) and the following constraints:

$$\begin{aligned} &\min OC\left(pH, H_2O_2, Fe^{2+}\right) \\ &s.t. \\ &DCOD \geq 40\% \\ &3 \leq pH \leq 6 \\ &9.7 \leq H_2O_2 \leq 38.82 \\ &0.7 \leq Fe^{2+} \leq 2.7 \end{aligned} \quad (20)$$

This optimization problem is a non-linear convex one, in a convex region which leads to infer that an overall global minimum exists within constrains. However, as the objective function for the OC (pH, H_2O_2, Fe^{2+}) is flat near its minimum value and discrete (because the minimum dollar denomination is 0.01 USD), multiple optimum values can be expected. Thus, the optimization problem, solved using different initial guesses for pH, $[H_2O_2]$ and $[Fe^{2+}]$, converged in the vast majority of the cases to the following values: pH = 4.33 and $[Fe^{2+}]$ = 1.14 mM. When varying $[H_2O_2]$ from 9.7 to 38.82 mM, at pH = 4.33 and $[Fe^{2+}]$ = 1.14 mM, OC changes are meaningfully (i.e., from 2.17 to

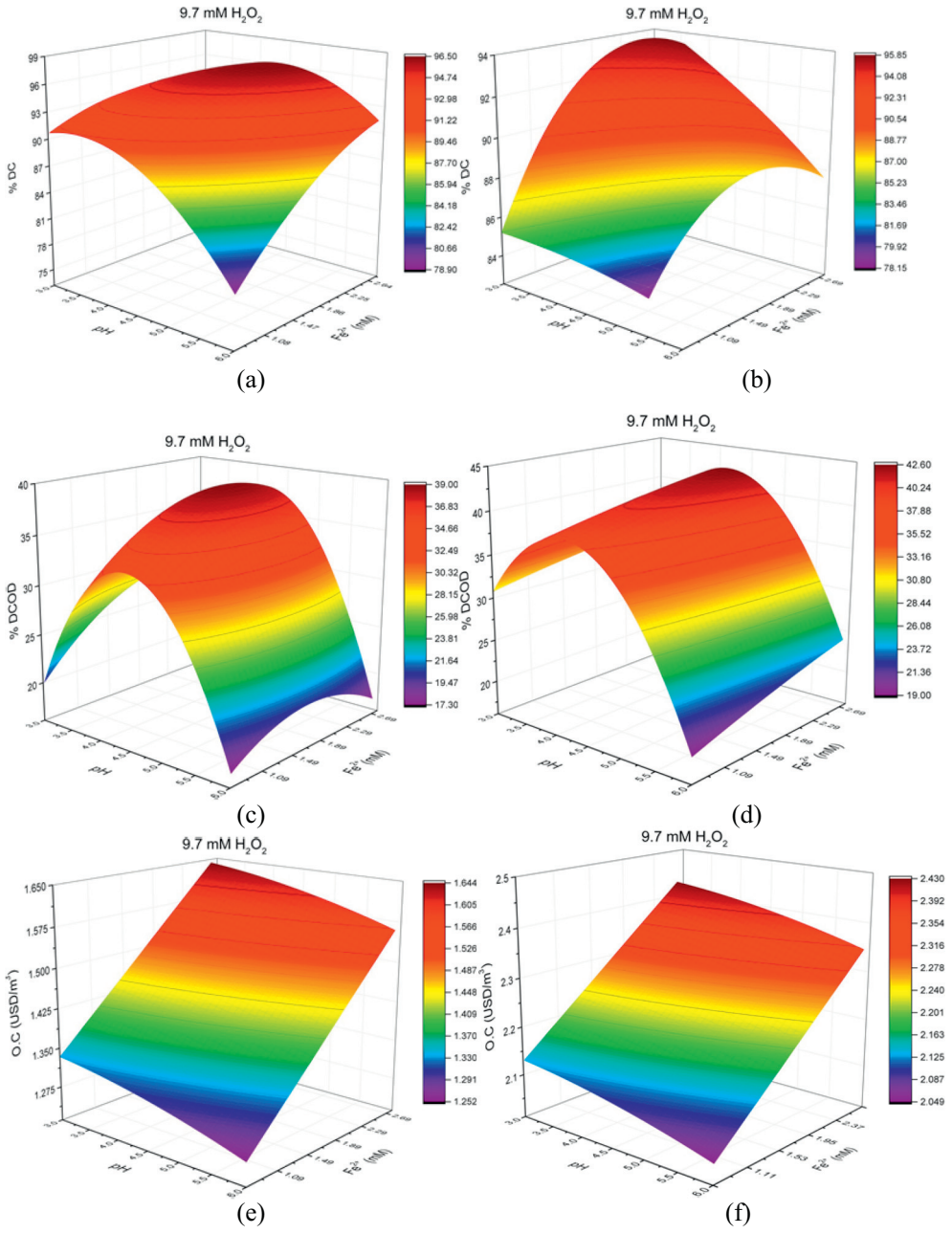

Fig. 2. Response surface diagrams for the interactive effect of [Fe^{2+}] and pH on %DC, %DCOD and OC for the F process ((a), (c), and (e)) and for PF process ((b), (d), (f)), respectively. Reaction time = 45 min., Temperature = 25 °C.

5.47 USD/m^3, respectively). Therefore, pH = 4.33, [Fe^{2+}] = 1.14 mM and [H_2O_2] = 9.7 mM were chosen as optimal conditions. This outcome is in agreement with the data reported by Cabrera-Reina et al. (2017) and Alalm et al. (2015).

The optimal conditions, obtained using BBD-RSM, were validated experimentally. The reactor's output was monitored during 70 min (i.e., EC = 10 min + F or PF = 60 min). The variations of %DC, %DCOD, %DTOC and OC as a function of time, during the sequential EC + F and EC + PF processes are presented in Fig. 3 and summarized in Table 1. Removal efficiencies and OC felt within the 95% prediction intervals, confirming the model's prediction capability. The dark blue color of wastewater completely vanished after 30 min. of F or PF. These results proved the decolorization effectiveness of F and PF processes, being in agreement with other reported studies (Maezono et al., 2011; Li et al., 2015). Color removal was faster than the COD and TOC ones, which implied that the chromophoric groups were easily damaged by the oxidation process. At the end of the treatment, COD removal reached ca. 274 mg/L with OC of 1.65 USD/m^3, and 238 mg/L and 2.3 USD/m^3 for EC + F and EC + PF processes, respectively. In both cases, Colombian permissible limits for the industrial wastewater discharges are fulfilled (COD <400 mg/L). The TOC removal efficiency was slightly lower than that of COD. TOC decreased from 220 mg/L to 55 mg/L and from 220 mg/L to 48 mg/L for EC + F and EC + PF, respectively. These results imply that part of the organic content in wastewater was degraded to other organic compounds and another great part was mineralized.

The BOD_5/COD ratio is customarily used for the assessment of physicochemical processes as a pretreatment before the biological ones. The BOD_5/COD ratio of raw wastewater was 0.21 (Table 1), indicating that the biodegradability of this wastewater was very low. This value increased up to ca. 0.27 after the EC process and then progressively up to ca. 0.42 and 0.46 after F and PF processes, respectively. These last

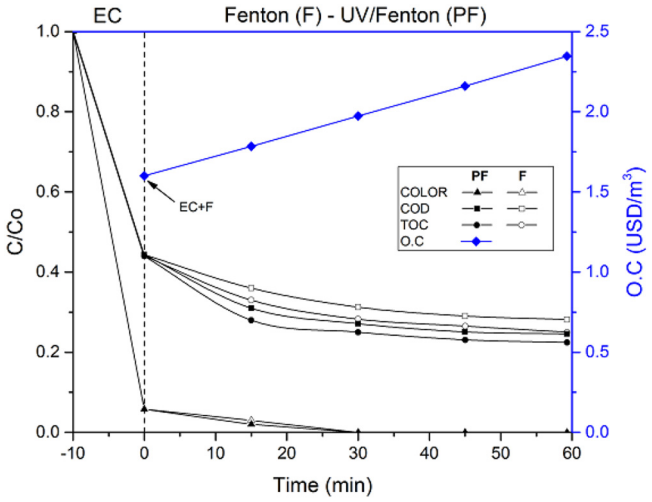

Fig. 3. The evolution of the color, COD and TOC removal and the OC of wastewater treated using EC + F or EC + PF process. Experimental conditions: EC process Fe anode and cathode, j_{EC} = 10 mA/cm^2, pH = 7, 60 rpm and 10 min of electrolysis time. F and PF processes: pH = 4.33, Fe^{2+} = 1.14 mM, H_2O_2 = 9.7 mM, and UV lamp 365 nm for PF.

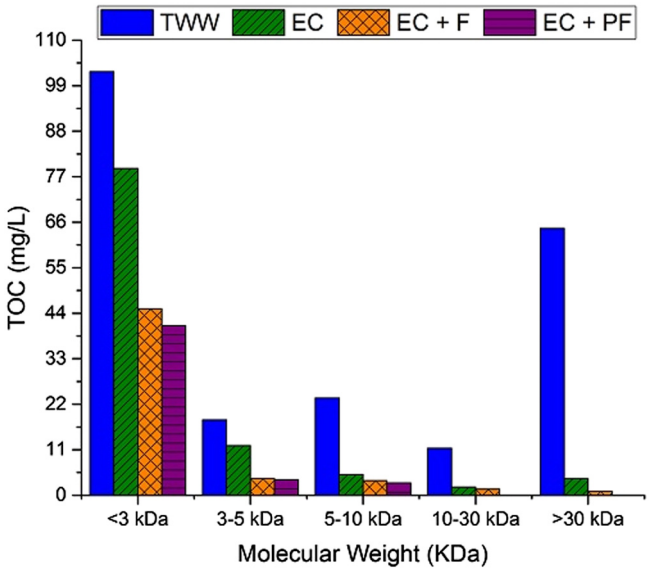

Fig. 4. MWD of raw and EC, EC + F and EC + PF effluent samples in terms of TOC. Experimental conditions: (i) EC process: Fe anode and cathode, j_{EC} = 10 mA/cm^2, pH = 7, 60 rpm and 10 min. of electrolysis time; (ii) F and PF processes: pH = 4.33, Fe^{2+} = 1.14 mM, H_2O_2 = 9.7 mM, UV lamp 365 nm for PF and 60 min of reaction time.

values imply that EC + F and EC + PF final effluent is biodegradable (BOD_5/COD ratio > 0.4).

3.3. Disposability of treated effluent

To get an idea of the possible fate of the organic pollutants, an effluent sample of each treatment was analyzed by spectrophotometry and HPLC. In addition, the molecular weight distribution (MWD) was also analyzed in the terms of TOC concentration and acute toxicity tests. For comparison, the raw wastewater sample was also analyzed using the same techniques. The UV–vis spectrum of raw wastewater sample (not shown here) consists of three main characteristic absorption bands: at 290 and 350 nm, which can be assigned to benzenic rings; and at 660 nm assigned to indigo dye (Workman Jr., 2001). After 30 min of F or PF reaction, these three peaks almost completely disappeared. It implies that some of the organic compounds were degraded/oxidized by the oxidant species (v.g., •OH, H_2O_2, HO_2•) generated during the F or PF processes.

MWD results are summarized in Fig. 4. The raw wastewater sample comprises primary compounds between 3 and 30 kDa due to the presence of large number of macromolecules (e.g., MW > 30 kDa = 29%: chemicals like surfactants, starch, waxes, oils, organic stabilizers, resins, carboxymethyl cellulose, etc.; MW < 3 kDa = 47%: formaldehyde, acids like acetic, formic, oxalic, etc.). EC + F and EC + PF processes effectively eliminated contaminants with MW in the range of 10–30 kDa. They were much more effective in TOC reduction for compounds with MW equal or higher than 5 kDa, reaching ca. 78% of TOC removal. However, in the case of compounds with MW equal or lower than 3 kDa, the final TOC concentration were very similar for after F and PF treatment completion. These findings are in agreement with previously published results (Brillas and Martínez-Huitle, 2015) reporting on the low efficiency of F and PF for oxidation of low molecular-weight carboxylic acids.

The evolution of representative four carboxylic acids (v.g., oxalic, maleic, formic and tartaric acids) were followed by ion-exclusion HPLC (Fig. 5). Maleic acid can be produced from the oxidative breaking of benzenic ring of aromatic byproducts, which are subsequently oxidized to malonic, oxalic, formic and tartaric acids (Oturan et al., 2008; Skoumal et al., 2008). Oxalic and formic acids are ultimate carboxylic acids since they are directly converted into CO_2. After 60 min. of EC + F and EC + PF treatments, 86.7 and 68.95 mg/L of malonic acid and 26.75 and 8.45 of oxalic acid, respectively, were detected (Fig. 5). Some residual formic and tartaric acids were also distinguished in the case of EC + F process.

Although the 60 min. of treatment could considerably reduce COD concentration to meet the Colombian emission limit values for industrial wastewater discharges (<400 mg/L), the toxicity of after-treatment wastewater should be verified (Fig. 6). The original wastewater is strongly toxic (i.e., 100% mortality) for *A. salina*. After EC process, wastewater toxicity remains unchanged. In fact, even though EC can effectively decolorize the wastewater, it still contains high COD concentration, residual chlorine/hypochlorite and toxic intermediates. On the other hand, although EC + F and EC + PF treatments were capable of degrading completely the dyes as well as reducing the total organic load (see Table 1), the final effluent was toxic (the mortality of *A. salina* decreased in 20% for EC + F and in 50% for EC + PF). This could be due to the presence of toxic intermediate by-products as well as secondary residual oxidants that remained in the reaction mixture (Li et al., 2015). Similar results were reported by Neamtu et al. (2003) who observed that the toxicity of azo dye C.I. Reactive Yellow 84 kept on decreasing during homogeneous photo-Fenton process, although toxic intermediates were formed in the initial stage of that treatment process. De Luna et al. (2014) also suggested that all the generated products of Orange II were less toxic than the original dye during homogeneous photo-Fenton process. Notice that the toxicity of EC + F + AC and EC + PF + AC processed effluents was negligible (ca. 15% and 0%, respectively). AC adsorption was able to remove chlorinated organic compounds and toxic intermediates. In fact, AC can react with free chlorine to produces oxygen-containing organic compounds on the carbon surface or CO_2 as the final product (Li et al., 2010).

4. Conclusions

In this study, a toxic and low biodegradable industrial textile wastewater, resulting from a denim manufacturing industry, was treated using sequential electrocoagulation + Fenton or Photo-Fenton + Activated carbon adsorption (EC + F/PF + AC) processes. At optimum operational conditions (pH = 4.33, H_2O_2 = 9.7 mM, Fe^{2+} = 1.14 mM and AC loading = 45 g), the sequential processes achieved total discoloration, COD reduction of 72 and 76%, and TOC mineralization of 75 and 78%, using F and PF processes, respectively. Additionally, the processes yielded a biodegradable effluent (i.e., BOD_5/COD equals to 0.42 (with

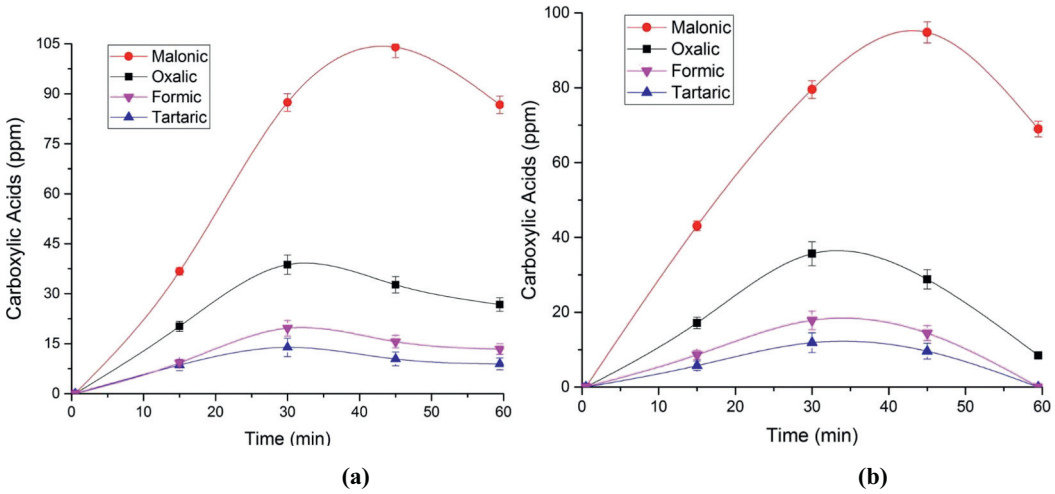

Fig. 5. Evolution of carboxylic acids generated during the degradation of ITWW by (a) EC + F and (b) EC + PF treatment under the same conditions of Fig. 3.

Fenton) and 0.46 (with PhotoFenton)). Bioassays, using *A. salina*, allowed assessing effluent toxicity. After 24 h-term exposure, brine shrimps mortality decreased from 100% for raw ITWW to 10 and 0% for EC + F + AC and EC + PF + AC treated effluents, respectively. The MWD analysis demonstrated that EC + F/PF + AC processes effectively decomposed contaminants with the MW in the range 10–30 kDa. A comprehensive operational cost analysis showed that the EC + F + AC process is more economic one (i.e., 1.65 USD/m^3). The coupled EC + F/PF + AC processes were demonstrated as efficient alternatives for the treatment of industrial effluents coming from denim tanning production.

Acknowledgements

The authors thank to the Dirección de Investigación de la Universidad EAFIT, Medellin–Colombia for financial support of this research. The staff of the Laboratorio de Ingeniería de Procesos is also recognized for their participation.

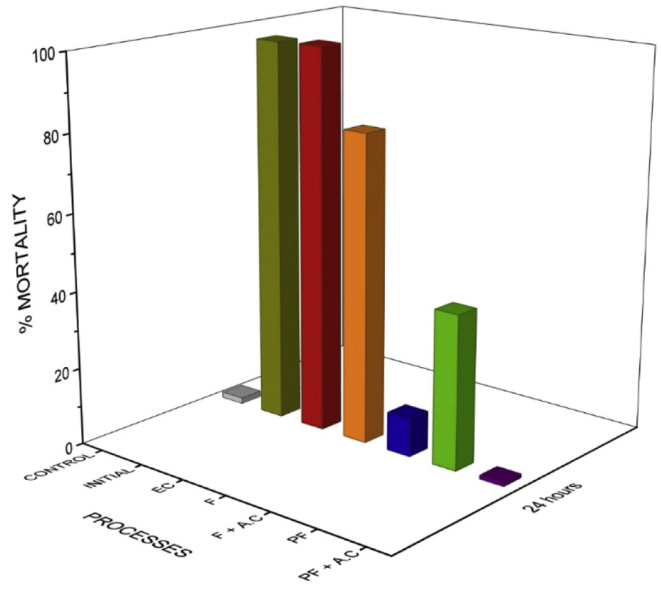

Fig. 6. Effect of each treatment process on effluent toxicity evaluated as the mortality percentage of *A. salina* after 24 h. EC, EC + F/PF under the same conditions of Fig. 3. AC adsorption conditions: flow rate = 20 mL/min, T = 25 °C, retention time = 3.7 min and AC loading = 45 g.

References

Alalm, M.G., Tawfik, A., Ookawara, S., 2015. Degradation of four pharmaceuticals by solar photo-Fenton process: kinetics and costs estimation. J. Environ. Chem. Eng. 3, 46–51.

APHA, WEF, 2012. Standard Methods for the Examination of Water and Wastewater. 22a ed. American Public Health Association, Washington.

Arzate-Salgado, S.Y., Morales-Perez, A.A., Solís-Lopez, M., Ramírez-Zamora, R.M., 2016. Evaluation of metallurgical slag as a Fenton-type photocatalyst for the degradation of an emerging pollutant: diclofenac. Catal. Today 266, 126–135.

Bautitz, I.R., Nogueira, R.F.P., 2007. Degradation of tetracycline by photo-Fenton process-solar irradiation and matrix effects. J. Photochem. Photobiol. A Chem. 187, 33–39.

Bobu, M., Yediler, A., Siminiceanu, I., Schulte-Hostede, S., 2008. Degradation studies of ciprofloxacin on a pillared iron catalyst. Appl. Catal. B Environ. 83, 15–23.

Boczkaj, G., Fernandes, A., 2017. Wastewater treatment by means of advanced oxidation processes at basic pH conditions: a review. Chem. Eng. J. 32, 608–633.

Brillas, E., Martínez-Huitle, C.A., 2015. Decontamination of wastewaters containing synthetic organic dyes by electrochemical methods. An updated review. Appl. Catal. B Environ. 166–167, 603–643.

Cabrera-Reina, A., Miralles-Cuevas, S., Casas López, J.L., Sánchez Pérez, J.A., 2017. Pyrimethanil degradation by photo-Fenton process: influence of iron and irradiance level on treatment cost. Sci. Total Environ. 605–606, 230–237.

Chatzisymeon, E., Xekoukoulotakis, N.P., Coz, A., Kalogerakis, N., Mantzavinos, D., 2006. Electrochemical treatment of textile dyes and dye house effluents. J. Hazard. Mater. 137, 998–1007.

Da Costa Filho, B.M., Da Silva, V.M., de Oliveira Silva, J., da Hora Machado, A.E., Trovo, A.G., 2016. Coupling coagulation, flocculation and decantation with photo-Fenton process for treatment of industrial wastewater containing fipronil: biodegradability and toxicity assessment. J. Environ. Manag. 174, 71–78.

Darvishi, R.C.S., Safari, M., Mashayekhi, M., 2016. Sonocatalyzed decolorization of synthetic textile wastewater using sonochemically synthesized MgO nanostructures. Ultrason. Sonochem. 30, 123–131.

De Lima, L.B., Pereira, L.O., de Moura, S.G., Magalhães, F., 2017. Degradation of organic contaminants in effluents—synthetic and from the textile industry—by Fenton, photocatalysis, and H_2O_2 photolysis. Environ. Sci. Pollut. Res. 24 (7), 6299–6306.

De Luna, L.A.V., Da Silva, T.H.G., Pupo Nogueira, R.F., Kummrow, F., Umbuzeiro, G.A., 2014. Aquatic toxicity of dyes before and after photo-Fenton treatment. J. Hazard. Mater. 276, 332–338.

Ding, Shaolan, Li, Zhengkun, Wangrui, 2010. Overview of dyeing wastewater treatment technology. Water Resour. Protec. 26, 73–78.

Domínguez, J.R., Gonzalez, T., Palo, P., Cuerda-Correa, E.M., 2012. Fenton + Fenton like integrated process for carbamazepine degradation: optimizing the system. Ind. Eng. Chem. Res. 51, 2531–2538.

El-Ghenymy, A., Garcia-Segura, S., Rodríguez, R.M., Brillas, E., El Begrani, S.M., Abdelouahid, B.A., 2012. Optimization of the electro-Fenton and solar photoelectro-Fenton treatments of sulfanilic acid solutions using a pre-pilot flow plant by response surface methodology. J. Hazard. Mater. 221–222, 288–297.

Emamjomeh, M.M., Sivakumar, M., 2009. Review of pollutants removed by electrocoagulation and electrocoagulation/flotation processes. J. Environ. Manag. 90, 1663–1679.

Flores, N., Brillas, E., Centellas, F., Rodríguez, R.M., Cabot, P.L., Garrido, J.A., Sirés, I., 2018. Treatment of olive oil mill wastewater by single electrocoagulation with different electrodes and sequential electrocoagulation/electrochemical Fenton-based processes. J. Hazard. Mater. 347, 58–66.

Garcia-Segura, S., Eiband, M.M., Vieira de Melo, J., Martínez-Huitle, C.A., 2017. Electrocoagulation and advanced electrocoagulation processes: a general review about the fundamentals, emerging applications and its association with other technologies. J. Electroanal. Chem. 801, 267–299.

Ghanbari, F., Moradi, M., 2015. A comparative study of electrocoagulation, electrochemical Fenton, electro-Fenton and peroxi-coagulation for decolorization of real textile wastewater: electrical energy consumption and biodegradability improvement. J. Environ. Chem. Eng. 3, 499–506.

GilPavas, E., Dobrosz-Gómez, I., Gómez-García, M.Á., 2017. Coagulation-flocculation sequential with Fenton or photo-Fenton processes as an alternative for the industrial textile wastewater treatment. J. Environ. Manag. 191, 189–197.

Ibarra Taquez, H.N., GilPavas, E., Blatchley III, E.R., Gómez-García, M.Á., Dobrosz-Gómez, I., 2017. Integrated electrocoagulation-electrooxidation process for the treatment of soluble coffee effluent: optimization of COD degradation and operation time analysis. J. Environ. Manag. 200, 530–538.

Jaafarzadeh, N., Ghanbari, F., Ahmadi, M., Omidinasab, M., 2017. Efficient integrated processes for pulp and paper wastewater treatment and phytotoxicity reduction: permanganate, electro-Fenton and Co_3O_4/UV/peroxymonosulfate. Chem. Eng. J. 308, 142–150.

Jorfi, S., Barzegar, G., Ahmadi, M., Soltani, R., Haghighifard, N., Takdastan, A., Saeedi, R., Abtahi, M., 2016. Enhanced coagulation-photocatalytic treatment of acid red 73 dye and real textile wastewater using UVA/synthesized MgO nanoparticles. J. Environ. Manag. 177, 111–118.

Kobya, M., Can, O.T., Bayramoglu, M., 2003. Treatment of textile wastewaters by electrocoagulation using iron and aluminum electrodes. J. Hazard. Mater. 100, 163–178.

Lemus, J., Martin-Martinez, M., Palomar, J., Gomez-Sainero, L., Gilarranz, M.A., Rodriguez, J.J., 2012. Removal of chlorinated organic volatile compounds by gas phase adsorption with activated carbon. Chem. Eng. J. 211–212, 246–254.

Li, B., Zhang, H., Zhang, W., Huang, L., Duan, J., Hu, J., Ying, W., 2010. Cost effective activated carbon treatment process for removing free chlorine from water. Asia Pac. J. Chem. Eng. 5, 714–720.

Li, H., Li, Y., Xiang, L., Huang, Q., Qiu, J., Zhang, H., Venkata, M., Fabien Baron, F., Barrault, J., Petit, S., Valange, S., 2015. Heterogeneous photo-Fenton decolorization of Orange II over Al-pillared Fe-smectite: response surface approach, degradation pathway, and toxicity evaluation. J. Hazard. Mater. 287, 32–41.

Maezono, T., Tokumura, M., Sekine, M., Kawase, Y., 2011. Hydroxyl radical concentration profile in photo-Fenton oxidation process: generation and consumption of hydroxyl radicals during the discoloration of azo-dye Orange II. Chemosphere 82, 1422–1430.

Malato, S., Fernandez-Ibañez, P., Maldonado, M.I., Blanco, J., Gernjak, W., 2009. Decontamination and disinfection of water by solar photocatalysis: recent overview and trends. Catal. Today 147, 1–59.

Mollah, M.Y.A., Morkovsky, P., Gomes, J.A.G., Kesmez, M., Parga, J., Cocke, D.L., 2004. Fundamentals, present and future perspectives of electrocoagulation. J. Hazard. Mater. 114, 199–210.

Neamtu, M., Yediler, A., Siminiceanu, I., Kettrup, A., 2003. Oxidation of commercial reactive azo dye aqueous solutions by the photo-Fenton and Fenton-like processes. J. Photochem. Photobiol. A 161, 87–93.

Oturan, M.A., Pimentel, M., Oturan, N., Sirés, I., 2008. Reaction sequence for the mineralization of the short-chain carboxylic acids usually formed upon cleavage of aromatics during electrochemical Fenton treatment. Electrochim. Acta 54, 173–182.

Pavoni, B., Drusian, D., Giacometti, A., Zanette, M., 2006. Assessment of organic chlorinated compound removal from aqueous matrices by adsorption on activated carbon. Water Res. 40, 3571–3579.

Rahim Pouran, S., Abdul Aziz, A.R., Wan Daud, W.M., 2015. Review on the main advances in photo-Fenton oxidation system for recalcitrant wastewaters. J. Ind. Eng. Chem. 21, 53–69.

Rosa, J.M., Fileti, A.M.F., Tambourgi, E.B., Santana, J.C.C., 2015. Dyeing of cotton with reactive dyestuffs: the continuous reuse of textile wastewater effluent treated by ultraviolet/hydrogen peroxide homogeneous photocatalysis. J. Clean. Prod. 90, 60–65.

Skoumal, M., Arias, C., Cabot, P.L., Centellas, F., Garrido, J.A., Rodríguez, R.M., Brillas, E., 2008. Mineralization of the biocide chloroxylenol by electrochemical advanced oxidation processes. Chemosphere 71, 1718–1729.

Vepsalainen, M., Kivisaari, H., Pulliainen, M., Oikari, A., Sillanpaa, M., 2011. Removal of toxic pollutants from pulp mill effluents by electrocoagulation. Sep. Purif. Technol. 81, 141–150.

Villanueva-Rodríguez, M., Hernández-Ramírez, A., Peralta-Hernández, J.M., Bandala, E.R., Quiroz-Alfaro, M.A., 2009. Enhancing the electrochemical oxidation of acid-yellow 36 azo dye using boron-doped diamond electrodes by addition of ferrous ion. J. Hazard. Mater. 167, 1226–1230.

Workman Jr., J., 2001. The Handbook of Organic Compounds. First edition. Academic Press, USA.

Yazdanbakhsh, A., Mehdipour, F., Eslami, A., Maleksari, H.S., Ghanbari, F., 2015. The combination of coagulation, acid cracking and Fenton like processes for olive oil mill wastewater treatment: phytotoxicity reduction and biodegradability augmentation. Water Sci. Technol. 71 (7).

Zazo, J.A., Casas, J.A., Mohedano, A.F., Gilarranz, M.A., Rodreguez, J.J., 2005. Chemical pathway and kinetics of phenol oxidation by Fenton's reagent. Environ. Sci. Technol. 39, 9295–9302.

Zazo, J.A., Pliego, G., Blasco, S., Casas, J.A., Rodriguez, J.J., 2011. Intensification of the Fenton process by increasing the temperature. Ind. Eng. Chem. Res. 50, 866–870.

Zhou, T., Lu, X., Wang, J., Wong, F.S., Li, Y., 2009. Rapid decolorization and mineralization of simulated textile wastewater in a heterogeneous Fenton like system with/without external energy. J. Hazard. Mater. 165 (1), 193–199.